applied sciences

MDPI

Article

The Influence and Compensation of Environmental Factors (pH, Temperature, and Conductivity) on the Detection of Chemical Oxygen Demand in Water by UV-Vis Spectroscopy

Jingwei Li *, Yipei Ding, Yijing Lu, Jia Liu, Chenxuan Zhou and Zhiyu Shao

School of Electrical, Energy and Power Engineering, Yangzhou University, No. 88 South University Road, Yangzhou 225009, China; mz120221197@stu.yzu.edu.cn (Y.D.); mz120231217@stu.yzu.edu.cn (Y.L.); mz120241257@stu.yzu.edu.cn (J.L.); mz120241273@stu.yzu.edu.cn (C.Z.); zhiyushao@yzu.edu.cn (Z.S.)
* Correspondence: jingwei_li@yzu.edu.cn

Abstract: In recent years, ultraviolet-visible (UV-Vis) spectroscopy has become one of the important methods used to measure water chemical oxygen demand (COD). However, environmental factors (pH, temperature, conductivity, etc.) can interfere with spectral information, thereby influencing the stability and accuracy of COD detection. The three environmental factors that influence UV-Vis spectroscopy were researched in this study. Considering the complexity of environmental factors, a data fusion method is proposed to compensate for the influence of three environmental factors simultaneously. This data fusion method is based on the weighted superposition of the spectrum and three environmental factors. A COD prediction model was established by fusing spectral feature wavelengths and environmental factors to reduce the influence of environmental factors on COD detection. Through the proposed data fusion method, the accuracy of COD detection based on UV-Vis spectroscopy has been improved. The determination coefficient of prediction (R^2_{Pred}) reaches 0.9602, and the root mean square error of prediction (RMSEP) reaches 3.52.

Keywords: UV-Vis spectroscopy; COD; environmental factors compensation; data fusion

check for updates

Academic Editors: Abdussalam Elhanashi and Pierpaolo Dini

Received: 11 December 2024
Revised: 24 January 2025
Accepted: 29 January 2025
Published: 7 February 2025

Citation: Li, J.; Ding, Y.; Lu, Y.; Liu, J.; Zhou, C.; Shao, Z. The Influence and Compensation of Environmental Factors (pH, Temperature, and Conductivity) on the Detection of Chemical Oxygen Demand in Water by UV-Vis Spectroscopy. *Appl. Sci.* **2025**, *15*, 1694. https://doi.org/10.3390/app15041694

Copyright: © 2025 by the authors. Licensee MDPI, Basel, Switzerland. This article is an open access article distributed under the terms and conditions of the Creative Commons Attribution (CC BY) license (https://creativecommons.org/licenses/by/4.0/).

1. Introduction

At present, spectroscopic detection technology is widely used in all walks of life, such as medicine and health [1,2], public safety [3,4], food safety [5], environmental monitoring [6–8], and so on. When a spectrum is used to detect chemical oxygen demand (COD), the quality of spectral data is crucial, as this is closely related to the accuracy of the COD prediction model. At the same time, different detection environments can also have a significant impact on the detection results [9–13]. COD detection based on the spectral method is the result of multiple environmental factors working together. Therefore, the question of how to eliminate environmental interference and extract effective spectral features is the key to improving the accuracy of spectral detection [14]. Environmental factors mainly include pH, temperature, conductivity, etc. Because UV-Vis spectroscopy belongs to the electronic energy spectrum. The acidity or alkalinity (pH) of a solution can affect the absorption peak position and absorption coefficient of the spectrum [15]. Temperature changes can alter the energy emission of electrons, thereby changing the waveform of the spectrum. Conductivity is mainly composed of soluble inorganic salt ions, some of which have strong absorption in the ultraviolet band. Therefore, addressing the influence of these

environmental factors is one of the important ways that the accuracy of COD detection by spectroscopic methods can be improved [16].

Changes in environmental factors (pH, temperature, and conductivity) cause certain interference to the spectrum when detecting COD in water with UV-Vis spectroscopy. This leads to the deviation of spectral data and influences the accuracy of COD detection. The influence of the environment on the detection of water parameters using spectroscopy methods has been researched, and corresponding compensation methods have also been proposed in some research. Katuhiro researched the relationship between COD and UV absorbance at 260 nm in the natural water of five rivers in Japan. He measured the absorbance of different inorganic salt ions in the water, indicating that inorganic salt ions have an influence on the spectroscopic detection of COD [17]. Croitoru used UV-Vis spectroscopy to detect nitrite and nitrate in the samples. It indicated that nitrite and nitrate have absorption in UV-Vis spectroscopy and can influence the absorption spectrum of COD [18]. Zhou et al. researched the effects of various environmental factors on the detection of COD in water by UV spectroscopy through standard solutions and real water samples. The influencing mechanism was analyzed, and relevant conclusions were drawn [19]. The influence of environmental factors on the full spectrum is quite complex. From a holistic perspective, it is not possible to simply fit the variation in absorbance with environmental factors at each wavelength using a single rule or curve. With the research on data fusion technology and its effectiveness in related fields, considering the fusing of different environmental factors with UV-Vis spectral data can achieve comprehensive compensation for the influence of environmental factors. Thus, the accuracy of COD detection based on UV-Vis spectroscopy is improved.

The water quality analysis methods of chemometrics have a development history of more than 50 years. However, the research method of combining spectroscopy with other forms of sensor data fusion has only been applied in recent years. It has problems such as poor robustness and low analysis accuracy [20]. Multi-source information fusion has its own characteristics and analysis methods when the data source to be fused includes spectral data [21]. According to different data sources, spectral fusion can be divided into two categories: the first is the fusion of different spectra, and the second is the fusion of spectra with other sensor data [22–24]. This research belongs to the second case. The fusion of spectroscopy with other sensors has been applied in many aspects. Cimander et al. used an electronic nose (EN), near-infrared spectroscopy (NIRS), and standard bioreactor probes to measure data to track the process of laboratory-scale yogurt fermentation. The sensor signals were fused by a cascade neural network. The results indicated that the fusion of online sensors with the selected analyzer can improve the monitoring and quality control of yogurt fermentation [25]. Casale et al. verified the geographical origin of extra virgin olive oil by an electronic nose and UV-visible spectrophotometer combined with multivariate analysis. The paper indicated that objective instrument data related to two important sensory characteristics, oil color, and aroma, could provide complementary information [26]. Pizarro et al. investigated the potential of visible fingerprints and physicochemical parameters and combined multivariate data analysis to classify extra virgin olive oil (EVOO) from different regions of Spain based on geographic sources. The results showed that after performing partial least squares discriminant analysis (PLS-DA) on the fusion matrix, the defined categories were perfectly distinguished, achieving 100% correct classification and a significant improvement in the overall prediction rate (92.5%) [27].

The application of fusion technology in the detection of water quality parameters is relatively limited. Qin et al. proposed using UV/Vis spectral fusion turbidity data to detect COD, TSS, oil, etc., in Chinese restaurant wastewater and using Boosting IPW-PLS to

establish a prediction model. The results indicated that the prediction model can effectively detect the water quality of wastewater, demonstrating the application prospects of data fusion technology for water quality detection [28]. Chen et al. researched the fusion of UV absorption spectra with different optical paths to detect COD in wastewater and established a prediction model based on data fusion using PLS. The results showed that compared with the standard measurement method, the residual prediction deviation (RPD) of the model was 3.72, and the R^2_{pred} was 0.936, demonstrating excellent predictive performance [29]. According to the literature that has been reviewed, there are currently few research reports on using spectral and other factors of fusion techniques for COD detection. The above work indicates that detection methods based on multi-source data fusion have higher prediction accuracy for COD detection than single-spectral methods.

Considering the complexity of the influence of environmental factors on water detection based on UV-Vis spectroscopy, this paper first presents the research conducted on the mechanism of the influence of environmental factors on UV-Vis spectroscopy. Then, research on multi-source data fusion algorithms is shown. Subsequently, research on multi-source data fusion modeling is presented. Finally, the COD prediction results of the model before and after the compensation of environmental factors are compared.

2. Materials and Methods

2.1. Samples Collection

The samples used in the experiment included a standard solution of COD and real water. The standard solution was obtained by diluting 1000 mg/L stock solution with distilled water in proportion. The real water was taken from Qianhu Lake in the center of Nanjing City. From June 2022 to June 2023, lake water samples were collected continuously for one year, with a sampling frequency of once a day (excluding holidays), and a total of 240 samples were obtained. Each collected water sample was divided into two parts, one measuring the standard values of water parameters and the other collecting UV-Vis spectroscopy data. To maintain the characteristics of the original water sample, relevant post-experiment procedures should be conducted immediately after water sample collection. Before the experiment, the water sample was not subjected to any other pre-treatment, such as filtration, to simulate the real situation of the water sample in the lake.

2.2. UV-Vis Spectrum Measurement

The UV-Vis spectrometer Cary 60 (Agilent, Santa Clara, CA, USA) was used to collect sample spectra, as shown in Figure 1. The spectrum range is from 193.91 nm to 1121.69 nm, with a resolution of 0.45 nm. The spectrometer is equipped with CaryWinUVV 5.0 (Agilent, Santa Clara, CA, USA) spectral acquisition software. The baseline correction is based on deionized water. The optical path length of the quartz cell is 10 mm. The integration time of the spectrometer is 10 ms. Each water sample was scanned 10 times in a row, and their average was noted. The original spectra of 240 collected water samples are shown in Figure 2.



Figure 1. UV-Vis spectra collecting equipment.

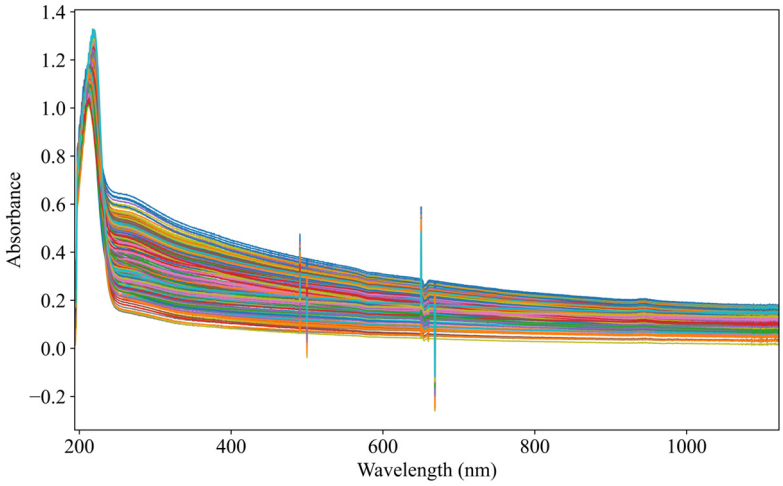


Figure 2. UV-Vis spectra of the different water samples (240 in total) collected from Qianhu Lake in the center of Nanjing City.

2.3. Standard COD Determination

The COD value of the samples was determined using rapid digestion spectrophotometry (HJ/T399-2007) [30,31]. The equipment used was the DRB200 digestive apparatus and DR3900 visible spectrophotometer (Hach, Loveland, CO, USA). The temperature of the DRB200 digestion tank was set to 150 °C, and the tank operated for 120 min.

2.4. Sample Set Division

The experiment included a total of 240 water samples. A total of 160 samples were randomly selected as the calibration set, and the remaining 80 samples were the prediction set. The statistical results of COD standard values for the samples are shown in Table 1. The COD standard values of the calibration and prediction set cover a wide range, which is beneficial to establishing a stable, accurate, and representative COD prediction model.

Table 1. COD standard values of 240 lake water samples.

Sample Set	Samples	Minimum (mg/L)	Maximum (mg/L)	Mean (mg/L)	Standard Deviation (mg/L)
Calibration	160	13.8	116.5	59.9	31.0
Prediction	80	16.1	116.1	59.6	31.2
All	240	13.8	116.5	59.7	31.1

2.5. Measurement of Environmental Factors in Water Samples

The influence of environmental factors on the determination of COD by UV-Vis spectroscopy was researched. The multi-factor portable measuring instrument SensION+MM156 (Hach, Loveland, CO, USA) was used to measure the pH, temperature, and conductivity of water. The statistical results of the environmental factor values of 240 water samples are shown in Table 2.

Table 2. The statistical results of the environmental factor values for 240 lake water samples.

Factors	Minimum	Maximum	Mean	Standard Deviation
pH	4.7	8.5	6.4	1.6
Temperature (°C)	0	33	15.5	9.8
Conductivity (mS/m)	0.2	137.7	11.4	45.8

2.6. Experimental Materials

To ensure that the water sample was not contaminated or altered during temporary storage, the samples were stored in a sealed glass bottle at room temperature to ensure the

reliability and accuracy of the experimental results. The water samples were used for the relevant experiments within 24 h of collection. All experimental materials were purchased from officially certified and legitimate stores. The reagents needed for the experiment were obtained by diluting high-concentration solutions. The solutions we purchased mainly included the 1000 mg/L potassium hydrogen phthalate solution, 1 mol/L $NaNO_3$, and potassium dichromate solution, 0.1 mol/L H_2SO_4 and NaOH solution, 0.5 g/mL mercury sulfate solution, 10 g/L silver sulfate solution, and distilled water. The test tubes and droppers, etc., used in the experiment were cleaned with ultrasonic waves and dried.

2.7. Data Modeling

Partial least squares (PLS) regression is one of the important modeling methods in spectral analysis. As a multivariate linear regression analysis technique, it is widely used in fields such as chemistry, environmental science, biomedicine, finance, etc., and performs particularly well in high-dimensional data and small sample problems [32–34]. The performance of PLS models is evaluated based on the root mean square error of calibration (RMSEC), the root mean square error of prediction (RMSEP), the coefficient of determination of calibration (R^2_{cal}), and the coefficient of determination of prediction (R^2_{pred}) [35,36]. The Python code used for modeling and analysis in this paper was modified based on the open-source programs available online. The main libraries used included Numpy for matrix operations, Pandas for data operations, Matplotlib for plotting, etc.

3. Experiment and Results Discussion

3.1. Effect of the Influence of Environmental Factors on UV-Vis Spectroscopy

3.1.1. Effect of the Influence of pH on UV-Vis Spectroscopy

The pH value of a water sample is used to indicate the acidity and alkalinity of the water. It is one of the most important physicochemical factors in water. It may lead to a series of water changes when the pH value changes, such as the ionization of some molecules, changes in molecular structure, and, thus, changes in the UV-Vis absorption spectrum of these molecules. In order to understand the influence of pH changes on COD detection based on UV-Vis spectroscopy, experiments were conducted on the influence of pH on COD detection. This section presents an experimental analysis of the influence of pH variations on the UV-Vis spectrum. To adjust the pH, 0.1 mol/L solutions of H_2SO_4 and NaOH were employed as pH regulators.

1. The influence of pH on the standard solution.

A 50 mg/L potassium hydrogen phthalate standard solution (COD standard solution) was prepared, exhibiting acidity with a pH of approximately four. To investigate the effect of pH, the pH of the standard solution was adjusted from 1.6 to 10.6 using an acid–base regulator. The UV-Vis spectra of these solutions are illustrated in Figure 3a. The absorbance curves at specific wavelengths (236.09 nm, 265.22 nm, and 280.46 nm) corresponding to the peaks and valleys in different pH ranges are illustrated in Figure 3b.

It can be seen from the spectroscopy of the standard solution in Figure 3a that, as the pH value increased, the absorbance gradually decreased, and a red shift phenomenon occurred in the absorption band. Above a pH of four, the rate of change in absorbance slowed, and the absorption band exhibited a blue shift. This phenomenon occurred because water, as a polar solvent, increases its polarity when the solution's pH rises, and OH^- ions neutralize some H^+ ions. This enhanced polarity induces a red shift in the $\pi \rightarrow \pi^*$ absorption band, slightly decreasing the molar absorption coefficient ε_{max}. Meanwhile, changes in pH may lead to alterations in the internal energy levels of molecules, such as enhanced intermolecular interactions and the increased rigidity of molecular structures. This increases the energy required for $n \rightarrow \pi^*$ transitions, resulting in a blue shift in the

absorption band. Figure 3b shows an overall decreasing trend in absorbance as the pH value increases. The absorbance at various wavelengths experiences a sharp decline at pH four. Although the absorbance continues to decrease above pH four, the decline is much slower. Below this pH value, the absorbance shows an overall decreasing trend as the pH value increases.

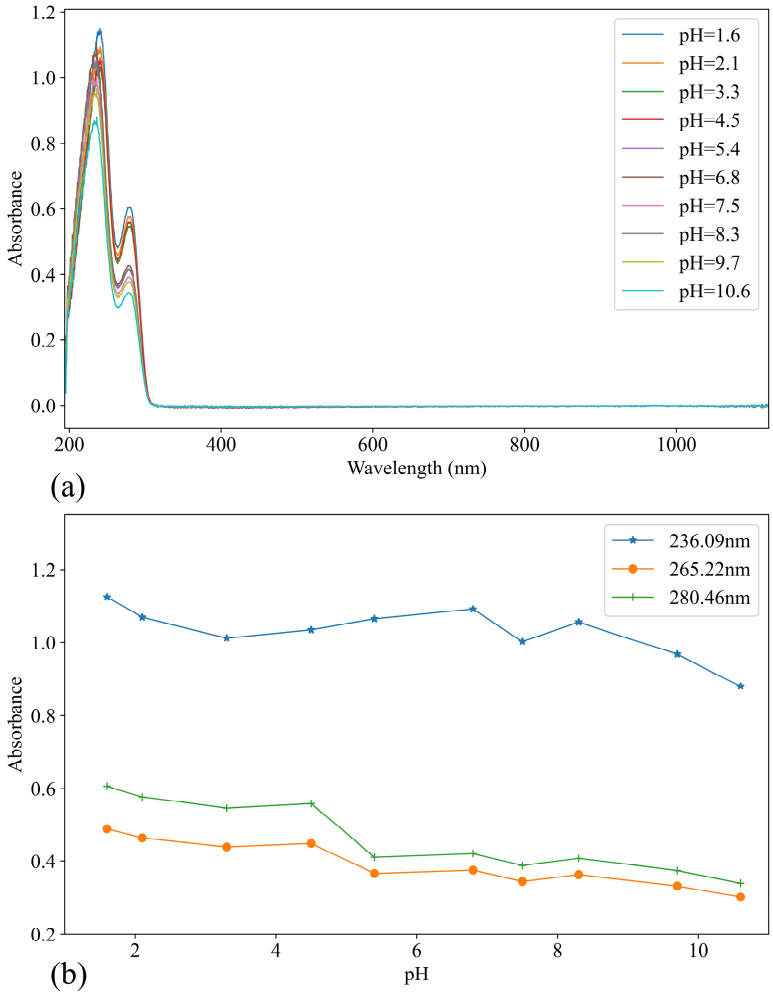


Figure 3. The influence of pH on the UV-Vis spectra of the standard solution. (**a**) The influence of pH on the UV-Vis spectra of the standard solution. (**b**) The change in absorbance at different wavelengths with the pH of the standard solution.

2. The influence of pH on real water samples.

A water sample with a COD concentration of 50.2 mg/L, as described in Section 2.1, was selected for the research. The pH of the water sample was adjusted from 1.3 to 10.8 using an acid–base regulator. The UV-Vis spectra of these water samples are illustrated in Figure 4a. The absorbance curves at the characteristic peaks and valleys (as identified in the COD standard solution) for different pH ranges are illustrated in Figure 4b.

Figure 4a shows the absorbance of lake water with a COD concentration of 50.2 mg/L, revealing a general decrease in absorbance as the pH increases. However, when the pH value is above four, a significant decrease in the overall trend is observed. This behavior can be attributed to the complex composition of the water sample, where the ionization of organic molecules is less affected under acidic conditions, leading to a relatively stable internal electronic structure. In contrast, under alkaline conditions, the further ionization of organic molecules occurs, altering their internal electronic structure, which induces polarization within the chromophore system and modifies the electronic states of organic

molecules. Consequently, this leads to changes in the spectral absorption band, with the absorption band broadening and the linear range decreasing as the pH becomes increasingly alkaline, ultimately affecting the absorbance. As shown in Figure 4b, the absorbance of the water sample has a spectral trend similar to that of the standard solution (as shown in Figure 3b).

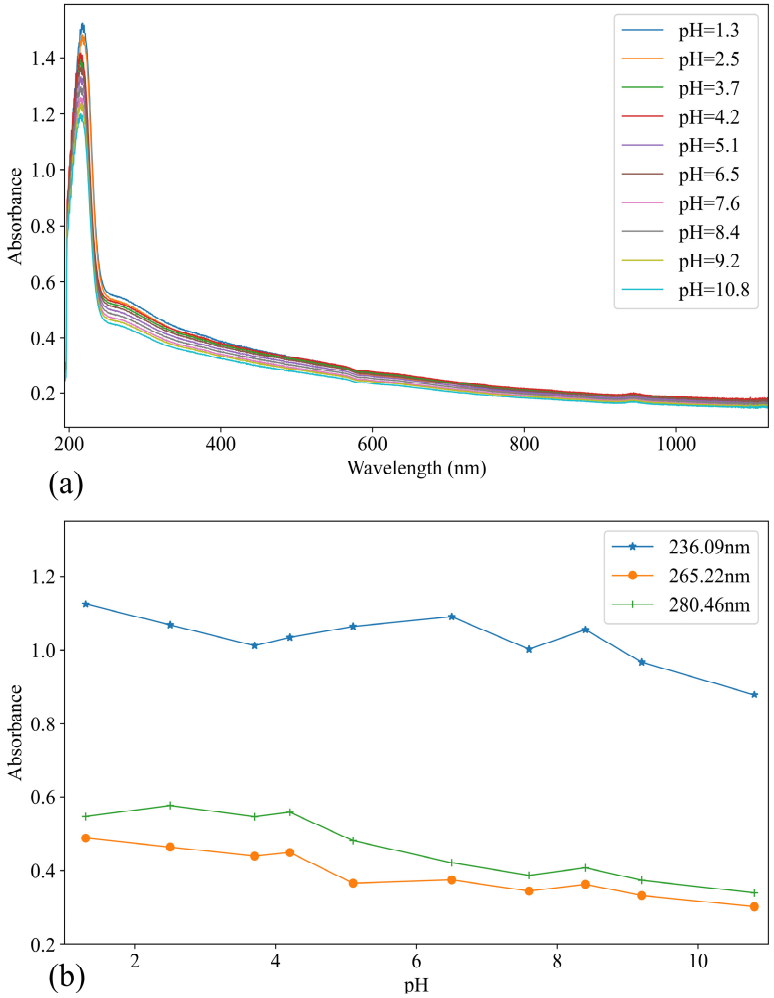


Figure 4. The influence of pH on the UV-Vis spectra of real water samples. (**a**) The influence of pH on the UV-Vis spectra of real water samples. (**b**) The change in absorbance at different wavelengths with the pH of real water samples.

From the above analysis, it is evident that the pH level has a minimal or unclear influence on UV-Vis spectroscopy when the pH ranges from one to four. However, when the pH value is above four, the overall trend of the UV-Vis spectrum will significantly shift downwards, accompanied by red and blue shifts. This indicates that the influence of pH on UV-Vis spectroscopy is not consistent across the entire pH range. Consequently, significant changes in the pH of a sample can introduce substantial errors in COD detection using UV-Vis spectroscopy. Given the wide range of pH variations in common surface waters, such as domestic sewage, rivers, and lakes, it is crucial to account for and compensate for the influence of pH to enhance the accuracy of COD detection.

3.1.2. Effect of the Influence of Temperature on UV-Vis Spectroscopy

The structure of molecules changes when the temperature rises, and the movement of molecules is closely related to temperature. The higher the temperature, the faster the movement of molecules in water, which inevitably influences COD detection. Moreover,

some devices in water detection, such as spectrometers and light sources, are also sensitive to temperature, all of which can influence UV-Vis spectroscopy. To investigate the influence of temperature on COD determination, an experiment was conducted on the influence of temperature on UV-Vis spectroscopy.

1. The influence of temperature on the standard solution.

The same 50 mg/L potassium hydrogen phthalate standard solution was prepared as that used in Section 3.1.1. The temperature of the solution was adjusted from 0 to 46.7 °C using a temperature-controlled chamber and ice. The UV-Vis spectra of these solutions are illustrated in Figure 5a. The absorbance curves of the characteristic peaks and valleys (as identified in the COD standard solution) at different temperature ranges are illustrated in Figure 5b.

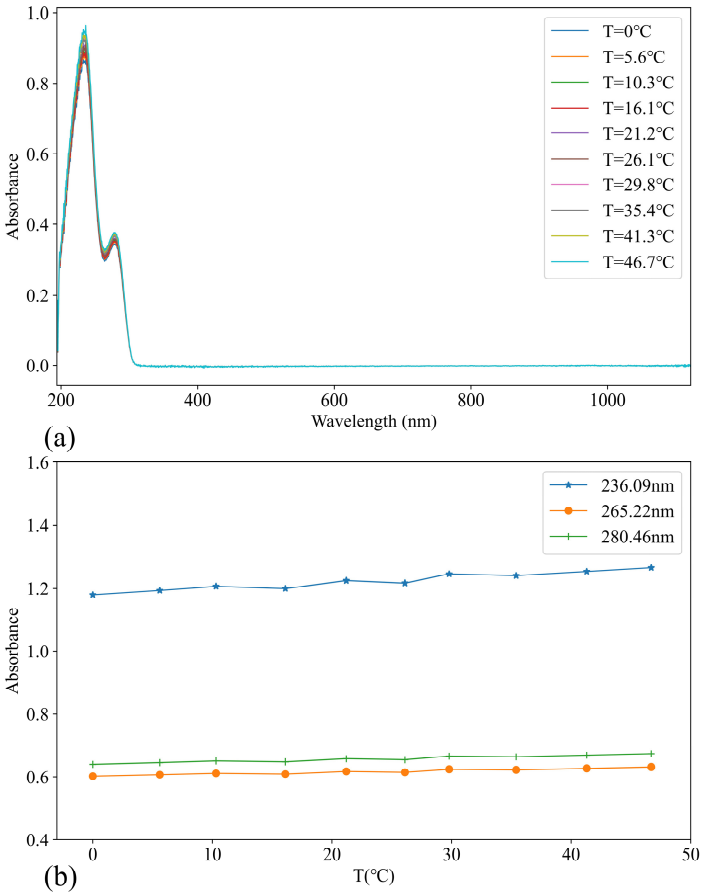


Figure 5. The influence of temperature on the UV-Vis spectra of standard solution. (**a**) The influence of temperature on the UV-Vis spectra of the standard solution. (**b**) The change in absorbance at different wavelengths with the temperature of the standard solution.

The UV-Vis absorption spectrum of the COD standard solution, as shown in Figure 4a, indicates that temperature changes have a measurable influence, with a variation of approximately 0.1 at the peak position of 236.09 nm. The absorbance demonstrates a positive correlation with increasing temperature. As shown in Figure 4b, the absorbance at different wavelengths also exhibits an upward trend, with a strong linear relationship to temperature. However, it is important to note that the linearity of the absorbance–temperature relationship varies across different wavelengths.

2. The influence of temperature on real water samples.

The composition of the water sample is more complex compared to the standard solution. Therefore, in this section, the lake water sample with a COD concentration of

50.2 mg/L, as described in Section 3.1.1, was selected for further analysis. The temperature of the lake water was adjusted from 0 to 47.2 °C using a temperature-controlled chamber and ice. The UV-Vis spectra of these water samples are illustrated in Figure 6a. The absorbance curves for the characteristic peaks and valleys (as identified in the COD standard solution) in different temperature ranges are illustrated in Figure 6b.

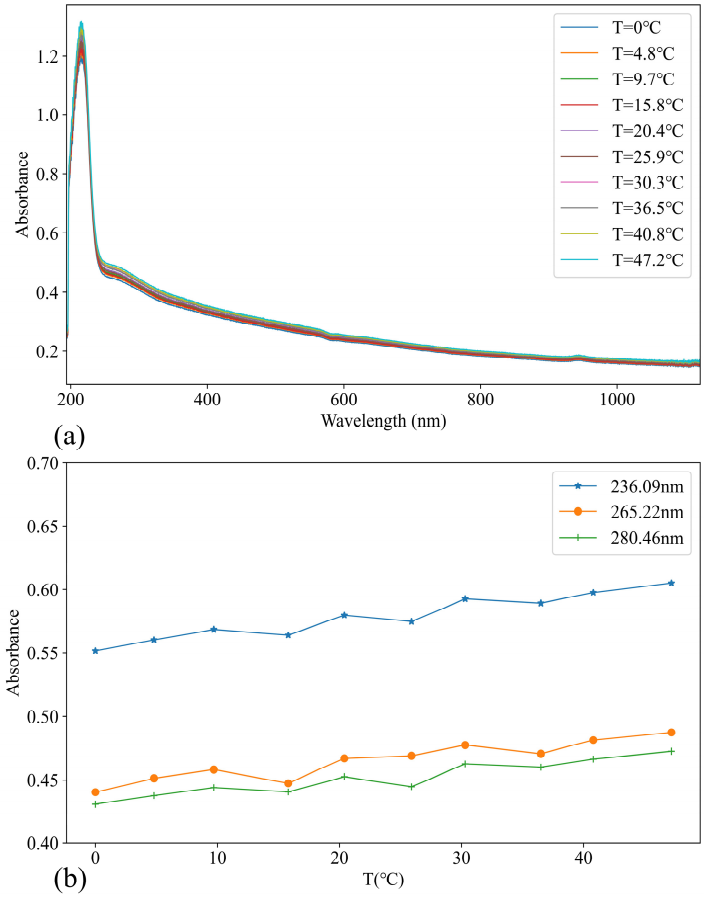


Figure 6. The influence of temperature on the UV-Vis spectra of real water samples. (**a**) The influence of temperature on the UV-Vis spectra of real water samples. (**b**) The change in absorbance at different wavelengths with the temperature of real water samples.

As shown in Figure 6a, the UV-Vis absorption spectrum of the real water samples also shows a temperature-induced change in absorbance of approximately 0.1 at the peak wavelength of 236.09 nm. The absorbance increases gradually, showing a positive correlation with rising temperatures. Furthermore, Figure 6b highlights a similar upward absorbance trend, as shown in Figure 5b, with greater clarity and prominence.

The above analysis demonstrates that temperature significantly impacts the UV-Vis spectrum of real water samples, generally exhibiting an approximately linear correlation. However, this linearity varies across different wavelengths, making the temperature's overall influence on the spectrum more complex. Consequently, it is challenging to accurately model temperature-induced absorbance changes at each wavelength using a simple curve. For COD detection based on UV-Vis spectroscopy, substantial temperature fluctuations can lead to significant errors. Given that temperatures in common surface waters, such as domestic sewage, rivers, and lakes, vary widely with seasonal and diurnal changes, compensating for the influence of temperature is essential to enhance the accuracy of COD detection.

3.1.3. Effect of the Influence of Conductivity on UV-Vis Spectroscopy

The conductivity of water is directly related to the concentration of dissolved salts or other inorganic substances capable of dissociating into electrolytes. The purer the water, the lower its conductivity. On the contrary, the higher the concentrations of compounds such as hydrochloric acid, nitrates, and sodium chloride, the higher the conductivity. Conductivity is influenced by several factors, including temperature, pH levels, and the concentration of inorganic pollutants. While pH indirectly influences the absorbance in UV-Vis spectra, certain inorganic ions exhibit strong absorption in the ultraviolet region, which can influence the accuracy of COD detection based on UV-Vis spectroscopy. This research specifically examines the influence of conductivity on UV-Vis spectra, using nitrate NO_3^- as a representative example.

1. The influence of NO_3^- on the standard solution.

Nitrite (NO_2^-) and nitrate (NO_3^-) in water are byproducts of the oxidation and decomposition of nitrogen-containing organic compounds and are eventually converted into NO_3^-. To investigate this, a COD concentration of 50 mg/L was prepared by mixing sodium nitrate ($NaNO_3$) solution with potassium hydrogen phthalate solution and adjusting the $NaNO_3$ concentration from 1 to 19 mg/L. The UV-Vis spectra of these solutions are illustrated in Figure 7a. The absorbance curves of the characteristic peaks and valleys (as identified in the COD standard solution) at different $NaNO_3$ concentrations are illustrated in Figure 7b.

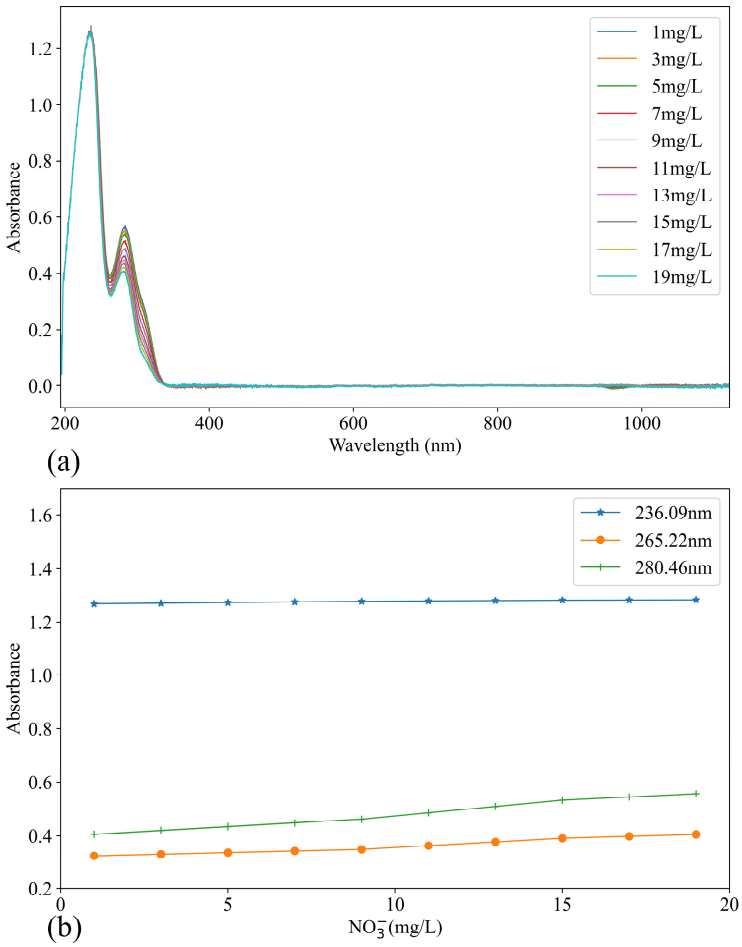


Figure 7. The influence of NO_3^- on the UV-Vis spectra of the standard solution. (**a**) The influence of NO_3^- on the spectra of the standard solution. (**b**) The change in absorbance at different wavelengths with the NO_3^- of the standard solution.

It can be seen from the spectroscopy of the COD standard solution in Figure 7a that NO_3^- shows obvious absorption peaks at around 280 nm and overlaps with one absorption peak of the COD standard solution. There is almost no absorption at the first absorption peak of the COD (236.09 nm). It can be observed that the absorbance increases by about 0.15 at the wavelength of 280 nm as the NO_3^- concentration gradually increases from 1 to 19 mg/L. It can also be observed that as the concentration of NO_3^- increases, the absorbance also increases (except at 236.09 nm), showing a good linear relationship in Figure 7b. However, the linear relationship corresponding to the absorbance at different wavelengths is inconsistent. Therefore, NO_3^- has a significant influence on UV-Vis spectroscopy. In order to eliminate its influence, a compensation method must be used in COD detection based on UV-Vis spectroscopy.

2. The influence of NO_3^- on real water samples.

The composition of real water samples is far more complex than that of standard solutions. Therefore, in this section, we continue to focus on the lake water sample with a COD concentration of 50.2 mg/L, as discussed in Section 3.1.1. The nitrate (NO_3^-) concentration in this water sample was adjusted from 0 to 19 mg/L. The UV-Vis spectra of these water samples are illustrated in Figure 8a. The absorbance curves at the characteristic peaks and valleys (as identified in the COD standard solution) for different $NaNO_3$ concentrations are illustrated in Figure 8b.

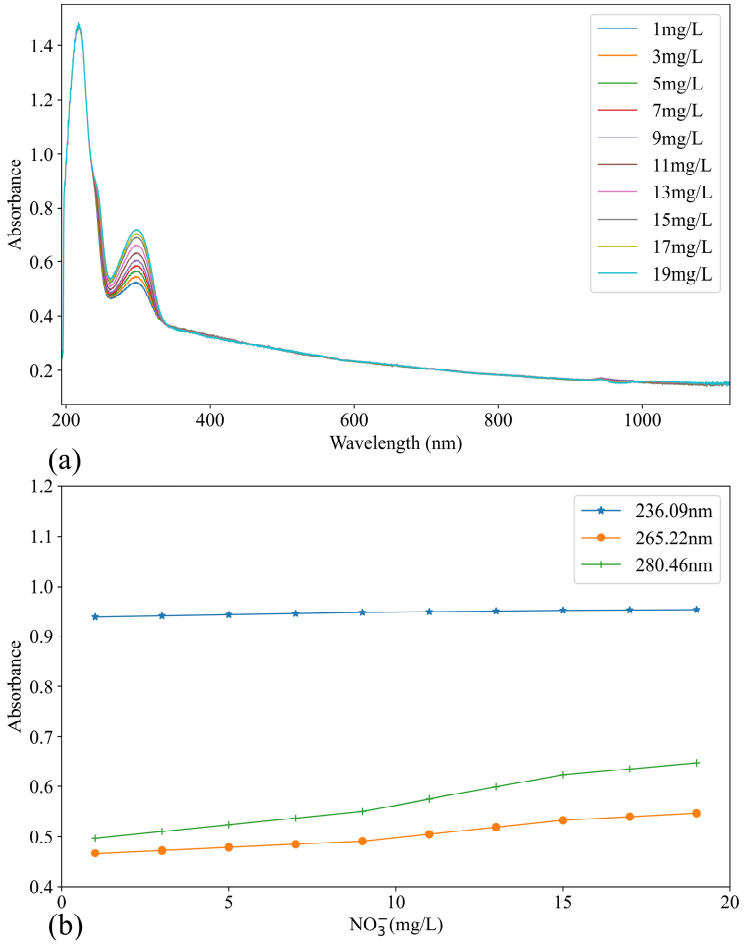


Figure 8. The influence of NO_3^- on the UV-Vis spectra of real water samples. (**a**) The influence of NO_3^- on the spectra of real water samples. (**b**) The change in absorbance at different wavelengths with the NO_3^- of real water samples.

The analysis of real water samples, as shown in Figure 8a, reveals that nitrate (NO_3^-) exhibits a distinct absorption peak at around 280 nm, which overlaps with one of the absorption peaks of the COD standard solution. There is minimal absorption at the first absorption peak of the COD at 236.09 nm. The absorbance at 280 nm increases by approximately 0.17 as the NO_3^- concentration increases from 1 to 19 mg/L. Furthermore, the absorbance generally increases with the rise in NO_3^- concentration (except for 236.09 nm), displaying a strong linear relationship, as shown in Figure 8b. However, the linearity of the absorbance at different wavelengths is inconsistent. Thus, NO_3^- significantly influences the UV-Vis spectroscopy, requiring the use of compensation methods to reduce this influence in COD detection based on UV-Vis spectroscopy.

From the analysis above, it is evident that conductivity has a significant and complex influence on the UV-Vis spectroscopy of real water samples, with considerable variations across different wavelengths. This complexity makes it challenging to accurately model the relationship between absorbance and conductivity through a simple curve or model. Consequently, the detection of COD based on UV-Vis spectroscopy can result in substantial errors when there are large fluctuations in the sample's conductivity. In the case of common surface waters, such as domestic sewage, rivers, and lakes, conductivity can vary widely with seasonal and environmental changes. Therefore, to enhance the accuracy of COD detection using UV-Vis spectroscopy, it is essential to compensate for the influence of conductivity.

3.1.4. Analysis of the Influence of Multiple Environmental Factors on UV-Vis Spectroscopy

Sections 3.1.1–3.1.3 provide a detailed analysis of the influence of individual environmental factors on UV-Vis absorption spectroscopy. However, in practical scenarios, the influence on detection is not due to a single environmental factor but is rather the result of the combined influence of multiple factors. Here, the combined influence of these environmental factors on the UV-Vis spectroscopy of both standard solutions and water samples, as discussed in Sections 3.1.1–3.1.3 is summarized in Table 3.

Table 3. Analysis of the influence of environmental factors on UV-Vis spectroscopy.

Environmental Factors	Influence Mode	Influence Level
pH	Red or blue shift, accompanied by upshift or downshift	The influence is significant, and the relationship is complex when the pH of the solution is high.
Temperature	Upshift or downshift	There is a certain influence, overall nonlinearity, and complex relationships.
Conductivity	Upshift or downshift	The influence is significant, and the relationship is complex.

The results from the experiments on the three environmental factors discussed in Sections 3.1.1–3.1.3 led to the following conclusions: water samples with varying pH levels induce red or blue shifts in the peaks and valleys of their UV-Vis spectra, accompanied by upward or downward shifts in absorbance. Temperature variations in water samples result in similar upward or downward shifts in the peaks and valleys of UV-Vis spectra. Additionally, changes in conductivity can cause shifts in these peaks and valleys. The influence of these environmental factors on the overall spectrum is intricate, and the absorbance at each wavelength cannot be fitted using a single rule or simple algorithm. Consequently, to enhance the accuracy of COD detection based on UV-Vis spectroscopy, it is essential to employ effective compensation methods to reduce the influence caused by these environmental factors.

3.2. COD Detection Compensation Based on Fusion of UV-Vis Spectroscopy and Environmental Factors

3.2.1. Data Fusion Theory

Data fusion, also known as information fusion, is a method that comprehensively evaluates data based on a certain fusion algorithm using the object or environment data obtained by multiple sensors. It involves the multi-level processing of multi-source data, including data detection, correlation, estimation, and combination. According to the degree of abstraction at the data processing level, data fusion can be divided into three levels: data-level fusion, feature-level fusion, and decision-level fusion [37].

The three fusion methods have different characteristics. Data-level fusion prediction is the fusion prediction that directly combines the raw data of various sensors in a certain way, belonging to the lowest level. The main advantage of this method is that it has the most real data, which is beneficial for further analysis and the processing of the data. However, this method has a large amount of data, so the processing time increases, and the real-time performance is poor. Feature-level fusion prediction is an intermediate-level type of fusion that extracts features from the raw data information of multiple sensors, combines them in a certain way, and finally comprehensively analyzes and predicts the target [38]. Feature-level fusion prediction effectively compresses the amount of information by extracting features from the original data, which is beneficial for real-time data processing [39]. Decision-level fusion prediction is the highest-level fusion prediction. Each sensor first establishes preliminary prediction models for the same target. Then, the results are combined in a certain way, and decision-level predictions are finally made. Decision-level fusion prediction has good real-time and fault tolerance, but its preprocessing cost is high [40].

Feature-level fusion takes into account the advantages and disadvantages of data-level fusion and decision-level fusion. To ensure the accuracy and real-time performance of data processing, this paper uses feature-level fusion to fuse spectral data and environmental factor data. Feature-level fusion refers to first extracting features from UV-Vis spectroscopy and preprocessing environmental factor data. Finally, fusion and modeling are performed. The process is shown in Figure 9.

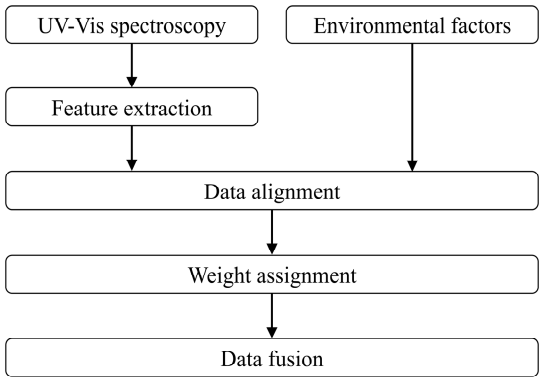


Figure 9. Feature-level fusion of UV-Vis spectroscopy and environmental factors.

3.2.2. Data Processing of UV-Vis Spectroscopy and Environmental Factors

The traditional view is that data fusion has a strong anti-interference ability and can incorporate complementary information from multiple sources of data. With in-depth research, the application of multi-source information fusion algorithms has been explored.

A better quantitative calibration model can be obtained using specific methods to select specific wavelength features. This enhances the predictive ability and robustness of the model. Therefore, selecting appropriate UV-Vis spectroscopy features and using their corresponding feature data as an input vector is very important.

1. Spectral data processing.

Firstly, the Stability Competitive Adaptive Reweighted Sampling (SCARS) algorithm is employed to extract features from the original spectral data. It is crucial to determine the optimal number of latent variables (LVs) for the PLS model in order to effectively filter the feature wavelengths using the SCARS algorithm. The initial maximum LV score for the PLS model is set to 15, and although the Monte Carlo sample count is set to 3000, this is not strictly necessary. The root mean square error of cross-validation (RMSECV) for PLS models across different LV values is illustrated in Figure 10. The minimum RMSECV value of 6.2604 occurs when the LV is nine, indicating that the optimal number of LVs for the PLS model is nine.

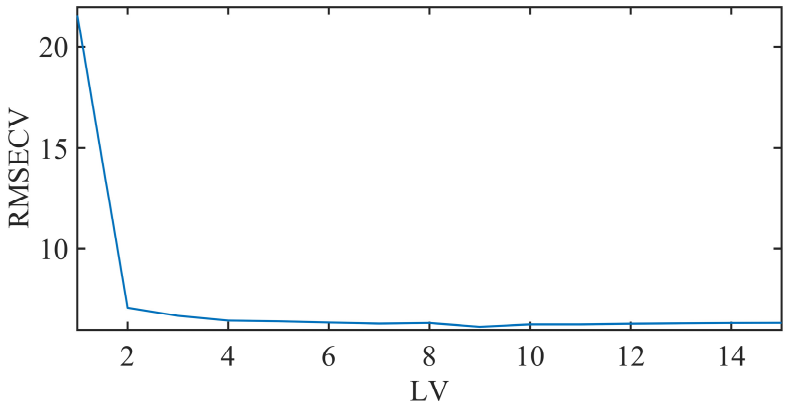


Figure 10. The variation curve of RMSECV with LV.

After multiple attempts to select suitable SCARS parameters, this paper sets the Monte Carlo sampling frequency to 200, the LV to nine, and the number of cross-validation groups to 10. It is shown that as the number of samples increases, the number of preferred wavelength variables gradually decreases in Figure 11. During the sampling process, from iterations 1 to 142, the RMSECV value continuously decreases, indicating that the variables removed during the filtering process are not related to COD. After 142 samples, as the number of samples increases, the RMSECV value begins to rise, indicating that the variables removed during the filtering process are related to COD, leading to an increase in the RMSECV value. Different colored lines represent the changes in regression coefficients for different iterations. The smallest RMSECV value (6.15) occurs when the sampling frequency reaches 142 times, and its corresponding subset of characteristic wavelengths is the best. This subset contains 14 wavelengths at 195.83 nm, 197.27 nm, 202.07 nm, 204.95 nm, 205.43 nm, 206.39 nm, 210.23 nm, 212.15 nm, 215.98 nm, 216.46 nm, 216.94 nm, 220.29 nm, 238.48 nm, and 241.35 nm, which are the optimal wavelength points after feature extraction using the SCARS wavelength selection method.

It can be seen that the highest absorbance value of UV-Vis spectroscopy occurs at around 1.4. However, the highest values of pH, temperature, and conductivity are 8.5, 33, and 137.7, respectively, from the actual UV-Vis spectroscopy shown in Figure 2 and the environmental factor data collected in Table 2. The spectral absorbance value is much smaller than the environmental factors value, and there is no comparability between them. If the spectral absorbance and environmental factor data are directly fused, the environmental factor data will play a dominant role in the model. The UV-Vis spectroscopy information is ignored, resulting in the failure of data fusion. Therefore, it is necessary to normalize the absorbance corresponding to fourteen wavelengths and three environmental factors before fusion (data alignment). In this way, two types of data are comparable at the same latitude, and then fusion, modeling, and other operations can be performed.

This paper uses min–max normalization ($\overline{x} = \frac{x - x_{min}}{x_{max} - x_{min}}$) to normalize spectral features and environmental factor data.

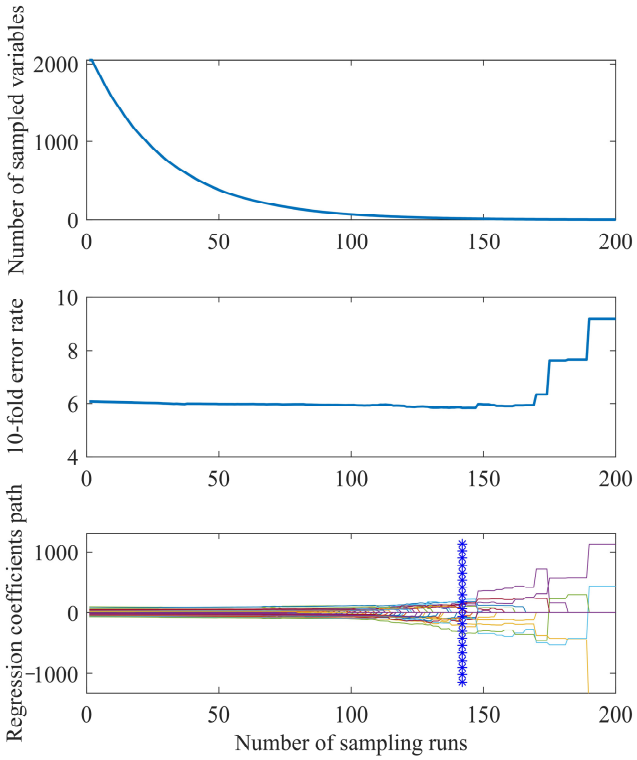


Figure 11. Process of feature extraction using SCARS method.

2. Environmental factor data processing.

Section 2.5 measured the environmental factors of the collected water samples and obtained pH, temperature, and conductivity data. Firstly, the max–min normalization ($\overline{x} = \frac{x - x_{min}}{x_{max} - x_{min}}$) is used to normalize environmental factors, and then the normalized data are used as the 15th-dimensional spectral absorbance data. In this way, data alignment is completed, and each type of data in data fusion is within a unified reference framework, and then feature-level data fusion modeling is performed.

3.2.3. Fusion Modeling of Spectra and Single Environmental Factor

After data processing, the PLS algorithm was used to establish a COD prediction model that fused spectral absorbance and a single environmental factor. The performance of the models is shown in Table 4.

Table 4. The model performance of compensation for single environmental factors.

Data Processing	Data Dimension	Calibration		Prediction	
		R^2_{cal}	RMSEC	R^2_{pred}	RMSEP
Raw spectrum + PLS	2048	0.8744	9.14	0.8481	10.86
SCARS + PLS	14	0.9138	6.56	0.8943	7.83
SCARS + pH + PLS	15	0.9485	4.29	0.9459	4.46
SCARS + Temperature + PLS	15	0.9177	6.30	0.9054	7.11
SCARS + Conductivity + PLS	15	0.9395	4.87	0.9317	5.39

It can be seen that the R^2_{pred} of the modeling results of the three environmental factors are pH, conductivity, and temperature in descending order from Table 4. Therefore, the order of influence of the three factors on the model is pH, conductivity, and temperature in descending order. It can be analyzed and understood from a chemical perspective that

pH causes a red shift and a blue shift in the spectral absorption curve, accompanied by an up- and downshift, thus having the greatest influence. The conductivity includes multiple components in water, which can cause significant interference in the detection of COD. Temperature needs to change over a large range to influence the spectroscopy data. In reality, temperature changes are within the room temperature range, and they have the lowest influence on the COD prediction model.

3.2.4. Fusion Modeling of Spectra and Three Environmental Factors

The actual COD detection does not come from the influence of a single environmental factor but from the combined influence of multiple environmental factors. Therefore, it is necessary to compensate for the influence of three environmental factors simultaneously. This paper proposes a fusion method based on the weighted superposition of spectra and three environmental factors in order to simultaneously compensate for the influence of three environmental factors. The weighted superposition method is shown in Formula (1). Here, x_{pH}, $x_{Temperature}$, and $x_{Conductivity}$ are the three environmental factors, and f_{pH}, $f_{Temperature}$, and $f_{Conductivity}$ are their corresponding weight coefficients. The three coefficients have been normalized, and their sum is one. The environmental factors are assigned corresponding weights (f_x) according to the value of R^2_{pred} in Table 4. The weight coefficients of pH, temperature, and conductivity were calculated according to Formulas (2)–(4).

$$\widetilde{x} = x_{pH} * f_{pH} + x_{Temperature} * f_{Temperature} + x_{Conductivity} * f_{Conductivity} \quad (1)$$

$$f_{pH} = \frac{R^2_{pH}}{R^2_{pH} + R^2_{Temperature} + R^2_{Conductivity}} \quad (2)$$

$$f_{Temperature} = \frac{R^2_{Temperature}}{R^2_{pH} + R^2_{Temperature} + R^2_{Conductivity}} \quad (3)$$

$$f_{Conductivity} = \frac{R^2_{Conductivity}}{R^2_{pH} + R^2_{Temperature} + R^2_{Conductivity}} \quad (4)$$

The weighted superposition of three environmental factors (WSTEFs) was taken as one factor $\widetilde{x}$. It was fused as the 15th dimension feature with the 14 features extracted by SCARS. The PLS model was established by the fusion of spectral features and WSTEF, and better COD detection accuracy was obtained. The R^2_{cal} of the model reached 0.9714, and RMSEC reached 2.19. The R^2_{pred} reached 0.9602, and RMSEP reached 3.52. The prediction results and standard value scatter plot of the COD prediction model based on SCARS+ WSTEF +PLS for the prediction set are shown in Figure 12. There is good consistency between the predicted values and the standard values.

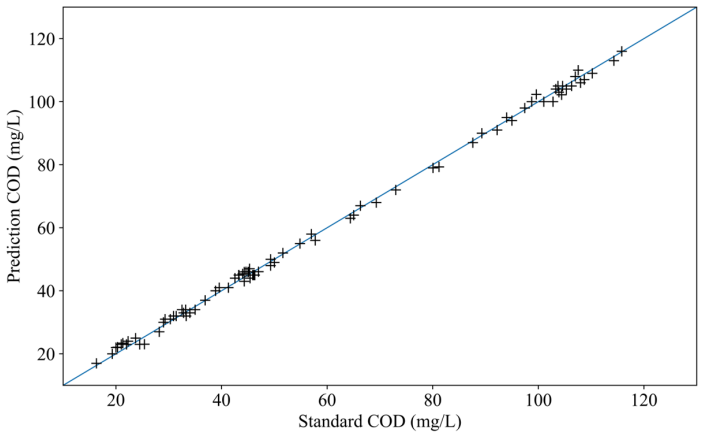


Figure 12. COD prediction results based on SCARS+ WSTEF +PLS.

3.3. Discussion

The UV-Vis spectroscopy used for COD detection in this research spans a spectral wavelength range from 193.91 nm to 1121.69 nm, with a spectral resolution of 0.45 nm, yielding a total of 2048 wavelength features. It may result in excessively high dimensionality for the input variables in the water COD prediction model using the full spectrum. This increases the complexity of the model and makes it prone to overfitting because the number of samples is significantly smaller than the number of spectral features. Consequently, the model's prediction accuracy is compromised, with an R^2_{pred} of just 0.8481 and an RMSEP of 10.86. Therefore, reducing the dimensionality of features is essential to simplifying the model and enhancing its predictive performance. The model had improved performance. R^2_{pred} increased to 0.8943, and the RMSEP decreased to 7.83. However, it is still a problem that environmental factors influence the UV-Vis spectroscopy, thereby influencing the stability and accuracy of COD detection. So, the influence of three environmental factors on UV-Vis spectroscopy was researched using a standard solution and real water samples. The mechanism of the influence of various environmental factors in water on UV-Vis spectroscopy was analyzed. Considering the complexity of the influence of environmental factors, data fusion was introduced to comprehensively compensate for the influence. Firstly, a COD prediction model based on the fusion of spectral characteristic wavelength and single environmental factor feature level was established to compensate for the influence of a single environmental factor. Through the fusion of spectral features and a single environmental factor, the accuracy of COD prediction was improved. Among the three factors, the pH single feature wavelength fusion model was the best, as the model's R^2_{pred} increased to 0.9459 and the RMSEP decreased to 4.46. However, the actual influence is not from a single environmental factor but the result of the interaction of multiple environmental factors. Therefore, a COD compensation model based on WSTEF was established, which combined spectral features and three environmental factors. The prediction accuracy of the model was further improved, and the optimal COD prediction model was obtained. The model's R^2_{pred} increased to 0.9602, and the RMSEP decreased to 3.52. Therefore, the fusion of UV-Vis spectroscopy and environmental factors achieved the more accurate detection of COD.

4. Conclusions

This paper mainly studies the influence of environmental factors on COD detection based on UV-Vis spectroscopy and the compensation method. Firstly, the influence of a single environmental factor on UV-Vis spectroscopy was analyzed through experiments. On this basis, the influence of multiple factors was also analyzed. Finally, data fusion technology was introduced to compensate for the influence of three environmental factors. This paper proposes a fusion method based on the weighted superposition of spectra and three environmental factors in order to simultaneously compensate for the influence of three environmental factors. In the first step, COD prediction models based on the fusion of spectral features and a single environmental factor were established, respectively. The results showed that the COD detection accuracy improved after the compensation of a single environmental factor. In the second step, a COD prediction model based on the WSTEF of three environmental factors and the feature-level fusion of spectral features was established. It further improved COD detection accuracy and obtained optimal COD prediction performance in this paper. Overall, the method of multi-source data fusion can significantly improve the COD detection accuracy based on UV-Vis spectroscopy.

Author Contributions: Software, Y.D.; Formal analysis, Y.L.; Investigation, J.L. (Jia Liu); Writing—original draft, C.Z.; Writing—review & editing, Z.S.; Supervision, J.L. (Jingwei Li). All authors have read and agreed to the published version of the manuscript.

Funding: This research received no external funding.

Data Availability Statement: The raw data supporting the conclusions of this article will be made available by the authors on request.

Acknowledgments: The authors would like to thank the editors and the reviewers for their helpful comments.

Conflicts of Interest: The authors declare no conflict of interest.

References

1. Li, L.; Pan, X.; Feng, Y.; Yin, L.; Hu, C.; Yang, H. Deep convolution network application in identification of multi-variety and multi-manufacturer pharmaceutical. *Spectrosc. Spectr. Anal.* **2019**, *39*, 3606–3613.
2. Li, X.; Feng, Y.; Duan, J.; Feng, L.; Wang, Q.; Ma, J.; Liu, W.; Yuan, X. Model-based mid-infrared spectroscopy for on-line monitoring of volatile fatty acids in the anaerobic digester. *Environ. Res.* **2022**, *206*, 112607. [CrossRef] [PubMed]
3. Nan, D.; Dong, L.; Fu, W.; Liu, W.; Kong, J. Fast identification of hazardous liquids based on Raman spectroscopy. *Spectrosc. Spectr. Anal.* **2021**, *41*, 1806–1810.
4. Rong, N.; Huang, M. Age Estimation of Bloodstains Based on Visible-Near Infrared Multi-Spectrum Combined Ensembling Model. *Spectrosc. Spectr. Anal.* **2020**, *40*, 168–173.
5. Yan, S.; Li, Y.; Peng, Y.; Ma, S.; Han, D. Detection of nitrofurans residues in honey using surface-enhanced Raman spectroscopy. *J. Food Sci.* **2022**, *87*, 3318–3328. [CrossRef] [PubMed]
6. Guan, L.; Zhou, Y.; Yang, S. An improved prediction model for COD measurements using UV-Vis spectroscopy. *RSC Adv.* **2024**, *14*, 193–205. [CrossRef]
7. Li, F.; Tang, B.; Zhao, M.; Hu, X.; Shi, S.; Zhou, M. Research on correction method of water quality ultraviolet-visible spectrum data based on compressed sensing. *J. Spectrosc.* **2021**, *2021*, 6650630. [CrossRef]
8. Guo, Y.; Liu, C.; Ye, R.; Duan, Q. Advances on Water Quality Detection by UV-Vis Spectroscopy. *Appl. Sci.* **2020**, *10*, 6874. [CrossRef]
9. Liu, E.; Wu, D.; Wang, J.; Tan, W.; Pu, J.; Luo, B.; Tang, B.; Long, Z.; Zhao, M. Multi-scene optimization method of water COD measurement based on direct spectroscopy. *Acta. Opt. Sin.* **2021**, *41*, 2230001.
10. Hu, Y.; Dai, B.; Yang, Y.; Zhao, D.; Ren, H. Sample Generation Method Based on Variational Modal Decomposition and Generative Adversarial Network (VMD–GAN) for Chemical Oxygen Demand (COD) Detection Using Ultraviolet Visible Spectroscopy. *Appl. Spectrosc.* **2023**, *77*, 1173–1180. [CrossRef] [PubMed]
11. Sheng, H.; Chi, H.; Xu, M.; Liu, S.; Wan, J.; Wang, J. Inland water chemical oxygen demand estimation based on improved SVR for hyperspectral data. *Spectrosc. Spectr. Anal.* **2021**, *41*, 3565–3571.
12. Zhou, K.; Bi, W.; Zhang, Q.; Fu, X.; Wu, G. Influence of temperature and turbidity on water COD detection by UV absorption spectroscopy. *Optoelectron. Lett.* **2016**, *12*, 461–464. [CrossRef]
13. Zhou, K.; Bai, X.; Bi, W. The Temperature, Turbidity and pH Impact Analysis of Water COD Detected by Fluorescence Spectroscopy. *Spectrosc. Spectr. Anal.* **2019**, *39*, 1097–1102.
14. Lv, Z.; Xiao, X.; Wang, Y.; Zhang, Y.; Jiao, N. Improved water quality monitoring indicators may increase carbon storage in the oceans. *Environ. Res.* **2022**, *206*, 112608. [CrossRef] [PubMed]
15. Chen, X.; Yin, G.; Zhao, N.; Yang, R.; Xia, M.; Feng, C.; Chen, Y.; Dong, M.; Zhu, W. Turbidity compensation method based on Mie scattering theory for water chemical oxygen demand determination by UV-Vis spectrometry. *Anal. Bioanal. Chem.* **2021**, *413*, 877–883. [CrossRef]
16. Post, C.; Brülisauer, S.; Waldschläger, K.; Hug, W.; Grüneis, L.; Heyden, N.; Schmor, S.; Förderer, A.; Reid, R.; Reid, M.; et al. Application of Laser-Induced, Deep UV Raman Spectroscopy and Artificial Intelligence in Real-Time Environmental Monitoring-Solutions and First Results. *Sensors* **2021**, *21*, 3911. [CrossRef] [PubMed]
17. Katuhiro, Y. Jrial of an organic compostion examination in natural water by UV spectram. *Chem. Edu.* **1999**, *47*, 338–341.
18. Croitoru, M.D. Nitrite and nitrate can be accurately measured in samples of vegetal and animal origin using an HPLC-UV/VIS technique. *J. Chromatogr. B* **2012**, *911*, 154–161. [CrossRef]
19. Zhou, K.; Liu, Z.; Cong, M.; Man, S. Analysis on influencing factors of detecting chemical oxygen demand in water by ultraviolet absorption spectroscopy. *Optoelectron. Lett.* **2022**, *18*, 749–754. [CrossRef]

20. Lyu, Y.; Zhao, W.; Kinouchi, T.; Nagano, T.; Tanaka, S. Development of statistical regression and artificial neural network models for estimating nitrogen, phosphorus, COD, and suspended solid concentrations in eutrophic rivers using UV-Vis spectroscopy. *Environ. Monit. Assess.* **2023**, *195*, 1114. [CrossRef] [PubMed]
21. Cao, Y.; Yang, W.; Li, H.; Zhang, H.; Li, M. Development of a vehicle-mounted soil organic matter detection system based on near-infrared spectroscopy and image information fusion. *Meas. Sci. Technol.* **2024**, *35*, 045501. [CrossRef]
22. Zou, M.; Liu, Y.; Fu, M.; Li, C.; Zhou, Z.; Meng, H.; Xing, E.; Ren, Y. Combining spectral and texture feature of UAV image with plant height to improve LAI estimation of winter wheat at jointing stage. *Front. Plant. Sci.* **2023**, *14*, 1272049. [CrossRef] [PubMed]
23. Zou, Y.; Zhang, A.; Wang, X.; Yang, L.; Ding, M. Comparison of feature selection and data fusion of Fourier transform infrared and Raman spectroscopy for identifying watercolor ink. *J. Forensic. Sci.* **2024**, *69*, 584–592. [CrossRef]
24. Huang, J.; Zhang, Y.; Yang, F.; Chai, L. Attention-Guided Fusion and Classification for Hyperspectral and LiDAR Data. *Remote Sens.* **2024**, *16*, 94. [CrossRef]
25. Cimander, C.; Carlsson, M.; Mandenius, C.F. Sensor fusion for on-line monitoring of yoghurt fermentation. *J. Biotechnol.* **2002**, *99*, 237–248. [CrossRef]
26. Casale, M.; Armanino, C.; Casolino, C.; Forina, M. Combining information from headspace mass spectrometry and visible spectroscopy in the classification of the Ligurian olive oils. *Anal. Chim. Acta.* **2007**, *589*, 89–95. [CrossRef]
27. Pizarro, C.; Rodríguez-Tecedor, S.; Pérez-del-Notario, N.; Esteban-Díez, I.; González-Sáiz, J.M. Classification of Spanish extra virgin olive oils by data fusion of visible spectroscopic fingerprints and chemical descriptors. *Food Chem.* **2013**, *138*, 915–922. [CrossRef]
28. Qin, X.; Gao, F.; Chen, G. Wastewater quality monitoring system using sensor fusion and machine learning techniques. *Water Res.* **2012**, *46*, 1133–1144. [CrossRef] [PubMed]
29. Chen, B.; Wu, H.; Li, S. Development of variable pathlength UV-vis spectroscopy combined with partial-least-squares regression for wastewater chemical oxygen demand (COD) monitoring. *Talanta* **2014**, *120*, 325–330. [CrossRef] [PubMed]
30. Dedkov, Y.; Elizarova, O.V.; Kel'ina, S.Y. Dichromate method for the determination of chemical oxygen demand. *J. Anal. Chem.* **2000**, *55*, 777–781. [CrossRef]
31. Rajkumar, D.; Palanivelu, K. Electrochemical treatment of industrial wastewater. *J. Hazard. Mater.* **2004**, *113*, 123–129. [CrossRef]
32. Qiu, J.; Guo, H.; Xue, Y.; Liu, Q.; Xu, Z.; He, L. Rapid detection of chemical oxygen demand, pH value, total nitrogen, total phosphorus, and ammonia nitrogen in biogas slurry by near infrared spectroscopy. *Anal. Methods* **2023**, *15*, 3902–3914. [CrossRef]
33. Hou, Y.; Zhang, A.; Lv, R.; Zhang, Y.; Ma, J.; Li, T. Machine learning algorithm inversion experiment and pollution analysis of water quality parameters in urban small and medium-sized rivers based on UAV multispectral data. *Environ. Sci. Pollut. Res.* **2023**, *30*, 78913–78932. [CrossRef]
34. Han, X.; Chen, X.; Ma, J.; Chen, J.; Xie, B.; Yin, W.; Yang, Y.; Jia, W.; Xie, D.; Huang, F. Discrimination of Chemical Oxygen Demand Pollution in Surface Water Based on Visible Near-Infrared Spectroscopy. *Water* **2022**, *14*, 3003. [CrossRef]
35. Zhou, K.; Liu, Z.; Cong, M.; Man, S. Detection of chemical oxygen demand in water based on UV absorption spectroscopy and PSO-LSSVM algorithm. Optoelectron. *Optoelectron. Lett.* **2022**, *18*, 0251–0256. [CrossRef]
36. Yao, L.; Shi, X.; Pan, T.; Chen, J. Wavelength Selection Method Based on Absorbance Value Optimization to Near-Infrared Spectroscopic Analysis. *Front. Phys.* **2021**, *9*, 663573. [CrossRef]
37. Wei, Y.; Wu, D.; Terpenny, J. Decision-Level Data Fusion in Quality Control and Predictive Maintenance. *IEEE. Trans. Autom. Sci. Eng.* **2021**, *18*, 184–194. [CrossRef]
38. Kim, H.; Lee, S.M.; Choi, S. Automatic sleep stages classification using multi-level fusion. *Biomed. Eng. Lett.* **2022**, *12*, 413–420. [CrossRef] [PubMed]
39. Wen, P.; Li, Y.; Chen, S.; Zhao, S. Remaining Useful Life Prediction of IIoT-Enabled Complex Industrial Systems With Hybrid Fusion of Multiple Information Sources. *IEEE. Internet Things J.* **2021**, *8*, 9045–9058. [CrossRef]
40. Alyahyan, S.; Wang, W. Decision level ensemble method for classifying multi-media data. *Wireless. Netw.* **2022**, *28*, 1219–1227. [CrossRef]

Disclaimer/Publisher's Note: The statements, opinions and data contained in all publications are solely those of the individual author(s) and contributor(s) and not of MDPI and/or the editor(s). MDPI and/or the editor(s) disclaim responsibility for any injury to people or property resulting from any ideas, methods, instructions or products referred to in the content.